Dust particle charging process in a radio frequency sheath of plasma containing kappa distribution electrons

Jing Ou [1],† and J.M. Long[1,2]

[1]Institute of Plasma Physics, Chinese Academy of Sciences, Hefei 230031, PR China

[2]University of Science and Technology of China, Hefei 230026, PR China

Based on self-consistent modelling of the radio-frequency sheath parameters, such as the ion and electron densities and the ion velocity, the dust particle charging process in an RF sheath is investigated by employing the kappa (κ) distribution for the electrons. It is shown that the charge number of the dust particle decreases near the sheath–wall interface while it shows the opposite tendency near the plasma-sheath edge, as the κ value is decreased. The fluctuation of the dust particle charge modified by the κ value depends on the dust particle radius. With an increases in the κ value, the fluctuation of the dust particle charge has a slight increase for a small dust particle, and it shows a significant increase for a large dust particle. In addition, as the κ value is decreased, the charge number of the dust particle obtained from the time-averaged plasma parameters deviates from the results obtained from the instantaneous plasma parameters. Moreover, a smaller deviation can be found for a large dust particle under the same κ value conditions.

---

1. Introduction

In a large variety of plasma applications, such as plasma processing and controlled fusion research, the dust particles mainly result from plasma–wall interactions and then enter the bulk plasma region across the sheath, which causes contamination in the plasma processing of integrated circuits and safety problems in fusion devices (Nitter 1996; Krasheninnikov, Smirnov & Rudakov 2011; Pustylnik *et al.* 2021). On the other hand, fine dust probes can be used to study plasma-sheath characteristics since the dust particles immersed in the plasma become charged by the action of electron and ion fluxes (Samarian & James 2001; Beadles, Wang & Horanyi 2017). Due to the importance of the dusty plasma in the sheath, numerous modelling related studies have been carried out, including the dust particle charging process and dynamics in both radiofrequency (RF) and static sheaths (Nitter 1996; Hou, Wang & Miskovic 2003; Bacharis, Coppins & Allen 2010; El Kaouini, Chatei & Bougdira 2014; Khalilpour & Foroutan 2020; Zhao, Zhang & Wang 2020).

† Email address for correspondence: ouj@ipp.ac.cn

For the dust particle charging process in an RF sheath, where quasi-neutrality breaks down and the large electric field gradients vary with time, Nitter introduced a model in which the electrons obey a Maxwellian distribution (Nitter 1996). Later, other authors studied the process in greater detail and addressed the issue of the determination of the dust particle charging process (Hou *et al.* 2003; Bacharis *et al.* 2010; El Kaouini *et al.* 2014; Missaoui, El Kaouini & Chatei 2021). However, the electron distribution in plasma discharges is not perfectly Maxwellian if the system of particles is in non-thermal equilibrium. The RF sheath of plasma containing non-Maxwellian electrons has been investigated recently (Ou, An & Men 2019; Ou & Huang 2020) and it is found that the supra-thermal electrons can modify the spatio-temporal variation of the plasma profile in the sheath region; such an effect of the non-Maxwellian electrons on the dust particle charge can be expected. According to the results of dust particles in a static sheath of non-Maxwellian plasma (Foroutan & Akhoundi 2012; Ou, Zhao & Lin 2018; El Ghani, Driouch & Chatei 2019; Khalilpour & Foroutan 2020; Zhao *et al.* 2020), it has been shown that the non-Maxwellian electrons can modify the profile of the dust particle when the dust components are relatively dense (Foroutan & Akhoundi 2012; El Ghani *et al.* 2019; Khalilpour & Foroutan 2020), while they can change the dust particle charging process and levitation when the dust density is very low (Ou *et al.* 2018; Zhao *et al.* 2020). Since the charge number of the dust particle in an RF sheath depends strongly on the RF field (Bacharis *et al.* 2010), the dust particle charging process in the non-Maxwellian electron RF sheath is more complex than in the static sheath. Here, we will discuss the effect of the supra-thermal electrons on the dust particle charging process by calculating the impact of both the instantaneous and time-averaged plasma parameters on the dust particles in the sheath.

Besides the electron distribution, we also relax some of restrictive assumptions involving the dust particle charging process in an RF sheath in this work in order to provide a wide extent of investigation. For example, it is assumed that the RF field frequency, ω_{RF}, is much larger than the ion plasma frequency ω_{pi} and smaller than the electron plasma frequency ω_{pe}, i.e. $\omega_{pi} \ll \omega_{RF} \ll \omega_{pe}$ (Nitter 1996; Bacharis *et al.* 2010; Shotorban 2012; El Kaouini *et al.* 2014). Under this condition, the ions respond only to the time-averaged electric field and the electrons follow the instantaneous RF field. To show the dust particle charge in an RF sheath with s wide range of frequency, we discuss a dust particle immersed in the sheath of a plasma obtained from a self-consistent model for the structure of the RF driven by a sinusoidal current source at the wall in the ion cyclotron range of frequency (ICRF) (Edelberg & Aydil 1999; Hou *et al.* 2003; Ou *et al.* 2018; Ou & Huang 2020). Apart from the RF field frequency, the dust particle radius is usually assumed to be much smaller than the local electron Debye length. Based on the Whipple approximation (Whipple 1981) and the neglect of the plasma screening, the dust particle charge can be calculated from the Debye–Hückel potential. For some applications, such as in a fusion plasma, however, the dust particle size limit no longer holds because the dust particle size can be up to tens of microns (Krasheninnikov *et al.* 2011; Zhang *et al.* 2021) while the local Debye length is relatively small due to the high plasma density. As a result, the Whipple approximation is only applicable in a limited range of dust size and the effect of the plasma screening on the dust particle charging must be taken into account. By using the model presented by Aussems *et al.* (2017), the modification of the effective screening length can be utilized to obtain the temporal evolution of the dust particle surface potential and the dust particle charge. In the present work, we take into account a dust particle radius comparable to or higher than the local Debye length under the tokamak plasma circumstance.

In the rest of this paper is organized as follows. Section 2 presents a one-dimensional model of the RF sheath containing supra-thermal electrons, which gives the profiles of the
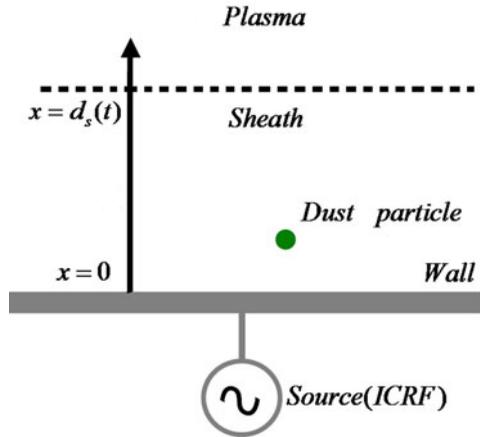
FIGURE 1. The geometry of the RF sheath model.

instantaneous and time-averaged plasma parameters, such as ion and electron densities and ion velocity. Section 3 concerns the effect of supra-thermal electrons on the dust particle charging process for different dust particle radii. Finally, the conclusions are drawn in § 4.

2. Sheath model

In the tokamak edge region, the plasma density n_s is usually 10^{17}–10^{18} m^{-3}, while the dust density is very low, e.g. only 10^4 m^{-3} in the DIII-D tokamak, and the charge number of a dust particle is 10^4–10^5 (Krasheninnikov *et al.* 2011). Therefore, we can assume that a dust particle is isolated and the dust particles do not contribute to the total space charge. As shown in figure 1, the RF sheath is formed in front of the wall where the current disturbance source in ICRF is set and the collisions in the sheath are neglected. For the sheath of plasmas containing only deuterium ions and non-Maxwellian electrons, the profile of the sheath potential $\phi(x, t)$ at any time t can be described by the Poisson equation

$$\frac{\partial^2 \phi}{\partial x^2} = -\frac{e}{\varepsilon_0}(n_i - n_e), \tag{2.1}$$

where e, ε_0, $n_i(x, t)$ and $n_e(x, t)$ are the elementary charge, permittivity of free space and ion and electron densities, respectively. At the wall position $x = 0$, the sheath potential $\phi(0, t) = \phi_w$. At the plasma-sheath edge $x = d_s$ where d_s denotes the sheath thickness, the sheath potential is approximately zero, i.e. $\phi(d_s, t) = 0$ and the plasma satisfies the quasi-neutral condition $n_{i,s} = n_{e,s} = n_s$.

The usual Maxwellian distribution cannot describe the tokamak edge plasma under some conditions such as in the presence of the supra-thermal electrons coming from edge heating by the wave. The kappa distribution is a generalization of the Maxwellian distribution and can be formed due to wave–particle interactions (Abid, Ali & Muhammad 2013). The power-law kappa (κ)-distribution function can be expressed as

$$f_\kappa(v) = \frac{n_s}{\sqrt{\pi \kappa \theta^2}} \frac{\Gamma(\kappa)}{\Gamma(\kappa - 1/2)} \left[1 + \frac{v^2}{\kappa \theta^2} \right]^{-(\kappa+1)}, \tag{2.2}$$

where Γ is the standard gamma function and $\theta = \sqrt{(\kappa - 3/2) 2 k_B T_e / \kappa m_e}$, with Boltzmann's constant k_B, the electron temperature for a Maxwellian distribution T_e and the

electron mass m_e. With the assumption of $\omega_{RF} \ll \omega_{pe}$, the electrons can instantaneously follow the RF field. By integrating over the κ-distribution velocity space, $n_e(x, t)$ is obtained (Hellberg *et al.* 2009)

$$n_e(x, t) = n_s \left[1 - \frac{e\phi(x, t)}{(\kappa - 3/2)k_B T_e} \right]^{-\kappa + 1/2}. \tag{2.3}$$

With the fluid approximation, $n_i(x, t)$ and the ion velocity, $v_i(x, t)$, are determined by the ion continuity and momentum equations

$$\frac{\partial n_i}{\partial t} + \frac{\partial (n_i v_i)}{\partial x} = 0, \tag{2.4}$$

$$\frac{\partial v_i}{\partial t} + v_i \frac{\partial v_i}{\partial x} = -\frac{e}{m_i} \frac{\partial \phi}{\partial x} - \frac{1}{m_i n_i} \frac{\partial p_i}{\partial x}, \tag{2.5}$$

here, m_i is the ion mass and the pressure term $p_i = n_i k_B T_i$ is for the isothermal approximation with ion temperature T_i. At the plasma-sheath edge, the ion velocity satisfies the Bohm criterion and $v_{i,s} = \sqrt{(T_{scr} + T_i)/m_i}$ for which the electron screening temperature $T_{scr} = (\kappa - 3/2)T_e/(\kappa - 1/2)$ can be obtained from $T_{scr} = en_e(\phi)/(dn_e/d\phi)|_{\phi=0}$.

By adopting the approach developed by Edelberg & Aydil (1999), the RF sheath is model as a parallel combination of a diode, a capacitor and a current source, and then an equivalent circuit model is used to close the system of equations to determine the relationship between the instantaneous d_s and ϕ_w by the following current balance equation at the wall:

$$eA_0[v_i(0, t)n_i(0, t) - \Gamma_e(0, t)] - I_d = I_{max} \sin(\omega t), \tag{2.6}$$

where A_0 is the wall area and the electron flux at the wall,

$$\Gamma_e(0, t) = n_s \sqrt{\frac{(\kappa - 3/2)T_e}{2\pi m_e}} \frac{\Gamma(\kappa - 1)}{\Gamma(\kappa - 1/2)} \left[1 - \frac{e\phi(0, t)}{(\kappa - 3/2)k_B T_e} \right]^{1-\kappa}. \tag{2.7}$$

The displacement current $I_d(t) = C_{cap}(d\phi_w/dt) + \phi_w(dC_{cap}/dt)$ with the time-dependent sheath capacitance $C_{cap} = \varepsilon_0 A_s/d_s$. The applied current disturbance source at the wall is assumed to be sinusoidal with amplitude I_{max}.

The system (2.1)–(2.6) is normalized with the following dimensionless quantities: $N_i = n_i/n_s$, $N_e = n_e/n_s$, $\varphi = e\phi/k_B T_e$, $u_i = v_i/\sqrt{k_B T_e/m_i}$, $d = x/\lambda_{D,i}$, $\tau_i = t/t_0$ with $t_0 = 2\pi/\omega_{pi}$. Where $\omega_{pi} = \sqrt{n_s e^2/m_i \varepsilon_0}$ and $\lambda_{D,i} = \sqrt{\varepsilon_0 k_B T_i/n_s e^2}$. With the sheath boundary conditions, we use the iteration method to solve numerically the set of closed nonlinear equations (2.1)–(2.6), and the iteration is repeated until the solutions converge to a self-consistent periodic steady state (Edelberg & Aydil 1999; Hou *et al.* 2003; Ou *et al.* 2019; Ou & Huang 2020). In this process, we can obtain the spatio-temporal distributions of the ion and electron densities, ion velocity and the sheath potential, and the corresponding time-averaged quantities, i.e. $\langle n_i(x)\rangle$, $\langle n_e(x)\rangle$, $\langle v_i(x)\rangle$ and $\langle \varphi(x)\rangle$ according to $\langle f(x)\rangle = \frac{1}{\tau}\int_0^\tau f(x, t)\, dt$ where $\tau = 2\pi/\omega_{RF}$ is the RF period. In our calculations, the RF sheath induced by the ICRF wave in a fusion plasma is considered with input parameters $\omega_{RF} = 50$ MHz and $I_{max} = 2000$ A, and deuterium discharge is taken into account as an example, with $T_i = T_e = 10$ eV, $n_s = 3.0 \times 10^{17}$ m^{-3}, $A_0 = 0.8$ m^2, as the typical parameters at an EAST-like tokamak during ICRF wave heating (Qin *et al.* 2015). With above parameters, $\lambda_{D,i} \approx 4 \times 10^{-5}$ m and $\omega_{pi} \approx 5 \times 10^{-8}$ s^{-1}.
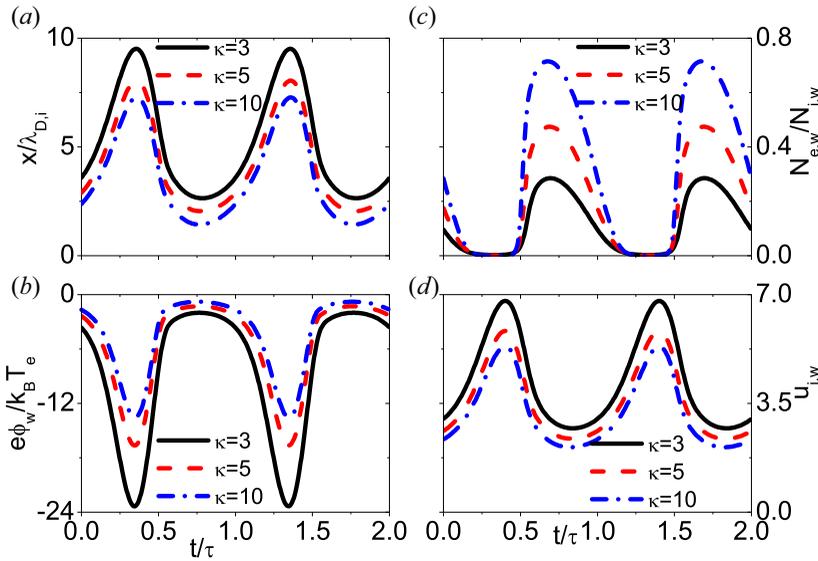
FIGURE 2. The normalized sheath length (*a*), sheath potential (*b*), ratio density of electron to ion (*c*) and ion velocity (*d*) in two cycles for the different κ values.

Figure 2 shows the variation of the sheath length, sheath potential drop, ratio density of electrons to ions and ion velocity near the wall with the time in two RF cycles for the different κ values. As the κ value is decreased, both the sheath length and the sheath potential drop, and the ion velocity near the wall increases, while the ratio of the density of the electrons and ions decreases. This is due to the fact that the decrease of the κ value implies an increase of the high electron energy tail in the electron velocity distribution. The electrons with higher energy can easily overcome the decelerating electric force and penetrate the sheath, and then reduce the net positive space charge and, consequently, broaden the sheath. From the variation of the sheath potential drop with the κ value, it is indicated that the RF field becomes strong when the supra-thermal electron component is present. The profiles of time-averaged ion and electron densities, ion velocity and the sheath potential are shown in figure 3. It is evident that the sheath length increases with the decrease of the κ value. For the same distance from the wall, the time-averaged ion and electron densities decrease while the ion velocity and sheath potential drop increase as the κ value is decreased. From figures 2 and 3, we may expect that the dust particle charging process can be modified by the κ value since the spatio-temporal variation of the sheath structure depends on the supra-thermal electrons.

3. Dust particle charging process

Dust particle charging is a dynamic process described by the charging equation

$$\frac{\mathrm{d}Q_d}{\mathrm{d}t} = I_{id} + I_{ed}, \tag{3.1}$$

where Q_d is the dust particle charge, I_{id} and I_{ed} are the currents of the ions and electrons from the plasma to the dust particle, respectively. When discussing the dust particle charging process immersed in a collisionless plasma, the most common approach is through the orbital motion limited (OML) theory. For the dust particles in tokamak edge plasmas, the charging time of a dust particle is much shorter than the characteristic time
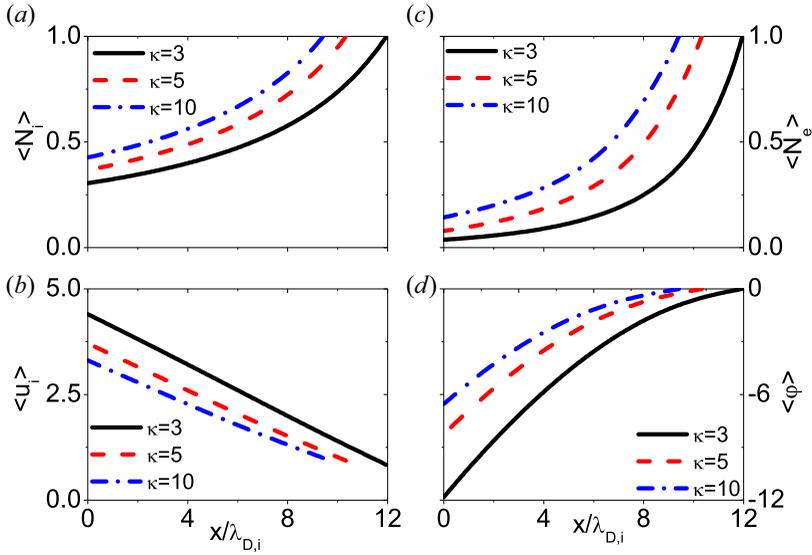
FIGURE 3. The normalized time-averaged sheath quantities as the function of the distance from the wall: the ion density (*a*), ion velocity (*b*), the electron density (*c*) and sheath potential (*d*) for the different κ values.

of dust particle transport (Krasheninnikov *et al.* 2011), and then the dust particle velocity relative to the ion velocity can be neglected in the charging process. Based on OML theory, the ion current to a spherical dust particle (Whipple 1981; Krasheninnikov *et al.* 2011)

$$I_{id} = \pi r_d^2 e n_i v_{ti} \left[\frac{v_i}{v_{ti}} erf\left(\frac{v_i}{v_{ti}}\right) + \frac{v_{ti}}{2v_i}\left(1 - \frac{2e\varphi_d}{k_B T_i}\right) erf\left(\frac{v_i}{v_{ti}}\right) + \frac{1}{\sqrt{\pi}} \exp\left(-\left(\frac{v_i}{v_{ti}}\right)^2\right)\right],$$
(3.2)

for a negative dust particle potential $\varphi_d < 0$ and

$$I_{id} = \frac{1}{2}\pi r_d^2 e n_i v_{ti} \left\{\left[\frac{v_i}{v_{ti}} + \frac{v_{ti}}{2v_i}\left(1 - \frac{2e\varphi_d}{k_B T_i}\right)\right][erf(u_{ip}) + erf(u_{im})]\right.$$
$$\left. + \frac{1}{\sqrt{\pi}}\frac{v_{ti}}{v_i}[u_{ip}\exp(-u_{im}^2) + u_{im}\exp(-u_{ip}^2)]\right\},$$
(3.3)

for s positive one.

The κ-distribution electron current to the spherical dust particle (Abid *et al.* 2013)

$$I_{ed} = -\pi r_d^2 e n_e \sqrt{\frac{8k_B[(\kappa - 3/2)/\kappa]T_e}{\pi m_e}} B_\kappa \left[1 - \frac{(\kappa - 1)e\varphi_d}{(\kappa - 3/2)k_B T_e}\right],$$
(3.4)

for a negative dust particle potential $\varphi_d < 0$ and

$$I_{ed} = -\pi r_d^2 e n_e \sqrt{\frac{8k_B(\kappa - 3/2)/\kappa T_e}{\pi m_e}} B_\kappa \left[1 - \frac{e\varphi_d}{(\kappa - 3/2)k_B T_e}\right]^{-\kappa+1},$$
(3.5)
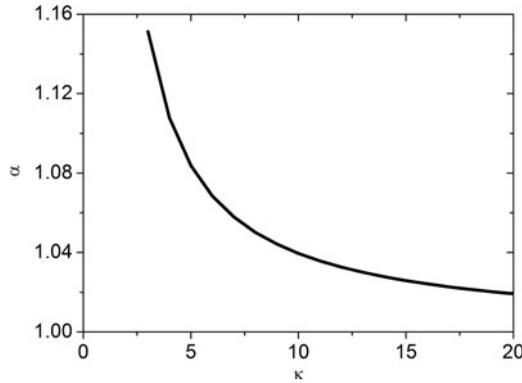
FIGURE 4. The variation of the factor α with the κ value.

for a positive one, where $v_{ti} = \sqrt{2k_B T_i/m_i}$ is the ion thermal speed and

$$u_{ip} = \frac{v_i}{v_{ti}} + \sqrt{\frac{2e\varphi_d}{k_B T_i}}, \quad u_{im} = \frac{v_i}{v_{ti}} - \sqrt{\frac{2e\varphi_d}{k_B T_i}}, \quad B_\kappa = \frac{\kappa}{\kappa^{3/2}(\kappa-1)} \frac{\Gamma(\kappa+1)}{\Gamma(\kappa-1/2)}. \quad (3.6a\text{--}c)$$

The relationship between Q_d and φ_d is given by $Q_d = C_0 \varphi_d$ (Whipple 1981). Where $C_0 = 4\pi\varepsilon_0 r_d(1 + r_d/\lambda_D)$ with $\lambda_D = (\lambda_{D,i}^{-2} + \lambda_{D,e}^{-2})^{-1/2}$ if $r_d < \lambda_D$, and $\lambda_D = (\lambda_{D,s}^{-2} + \lambda_{D,e}^{-2})^{-1/2}$ if $r_d > \lambda_D$. The electron Debye length $\lambda_{D,e} = \sqrt{\varepsilon_0 k_B[(\kappa - 3/2)/\kappa]T_e/n_s e_0^2}$ and the effective screening length $\lambda_{D,s} = \sqrt{1 + 0.48\sqrt{\beta_s}}\lambda_{D,i}$, with $\beta_s = (e\varphi_d/k_B T_e)([(\kappa - 3/2)/\kappa]T_e/T_i)(r_d/\lambda_{D,i})$ (Aussems *et al.* 2017).

Linearizing (3.1) around an equilibrium charge $Q_{d,\text{eq}}$, we can obtain (Melandsø *et al.* 1996; Nitter 1996)

$$\frac{dQ_{d,1}}{dt} = \left(\frac{\partial(I_{id} + I_{ed})}{\partial Q_d}\right)_{Q_{d,\text{eq}}} Q_{d,1}, \quad (3.7)$$

where $Q_{d,1}$ is a small perturbation from $Q_{d,\text{eq}}$. Equation (3.7) has the solution $Q_{d,1} = Q_{d,0} \exp(-\omega_{\text{ch}}t)$ with the initial perturbed charge $Q_{d,0}$ and the characteristic charging frequency $\omega_{ch} = -(\partial(I_{id} + I_{ed})/\partial Q_d)_{Q_{d,\text{eq}}}$. The characteristic charging time $\tau_{\text{ch}} = 1/\omega_{\text{ch}}$. Based on (3.2)–(3.5), we can obtain the rough dependence of τ_{ch} on the plasma parameters and dust particle radius

$$\tau_{\text{ch}} \propto \frac{\alpha\sqrt{T_e}}{r_d n_s}, \quad (3.8)$$

here, $\alpha = \kappa^{3/2}\Gamma(\kappa - 1/2)/\Gamma(\kappa + 1)$ is defined as a factor set to characterize the effect of the κ value. The dependence of the α value on the κ value is shown in figure 4. From the small κ value corresponding to the large α value, it is indicated that the supra-thermal electrons can increase τ_{ch}. The α value tends to 1 as the κ value is increased, and the resultant τ_{ch} or ω_{ch} tends to approach the Maxwellian electron case (Nitter 1996).

Here, a dust particle with $1\,\mu\text{m} < r_d < 50\,\mu\text{m}$ is investigated based on $\lambda_{D,i} \approx 40\,\mu\text{m}$ calculated from the numerical parameters mentioned in the above section. For the sake of discussion, the following quantities are also defined. The charge number of a dust particle $Z_d = |Q_d/e|$. The time-averaged charge of a dust particle and charge number in an RF period are $\langle Q_d \rangle = \frac{1}{\tau}\int_0^\tau Q_d(t)\,dt$ and $\langle Z_d \rangle = \frac{1}{\tau}\int_0^\tau Z_d(t)\,dt$, respectively. The root-mean-square of the charge number $Z_d^{\text{RMS}} = \sqrt{\frac{1}{\tau}\int_0^\tau (Q_d/e)^2\,dt}$. The root-mean-squared
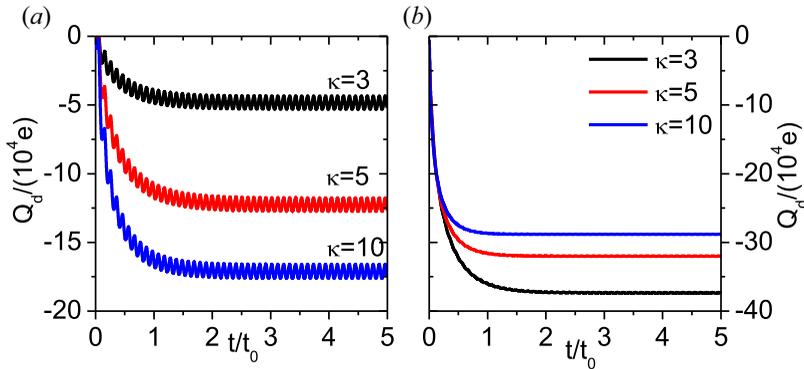
FIGURE 5. The evolution of the dust particle charge as a function of time for the different κ values with $r_d = 10\ \mu$m near the sheath–wall interface (*a*), and at the plasma-sheath edge (*b*).

error $Z_d^{\mathrm{RMSE}} = \sqrt{\frac{1}{\tau} \int_0^\tau (Q_d/e - \langle Q_d \rangle/e)^2\, \mathrm{d}t}$, which is a quantity representing the scale of fluctuations of the dust particle charge, and the $\Delta Z_d^{\mathrm{amp}} = |Q_d^{\mathrm{max}}/e - Q_d^{\mathrm{min}}/e|/2$ which indicates the RF amplitude (Shotorban 2012). The above corresponding quantities associated with φ_d also can be obtained based on $Q_d = C_0 \varphi_d$.

Figure 5 shows the charging relaxation process of a dust particle for the different κ values near sheath–wall interface and plasma-sheath edge. Near the sheath–wall interface, the charge number of the dust particle ($Z_d = |Q_d/e|$) increases rapidly with increasing time, and then reaches a quasi-stationary state with oscillation due to the strong RF field. The charging relaxation time of a dust particle with $r_d = 10\ \mu$m is approximately $3 \times 2\pi/\omega_{\mathrm{pi}} = 2.04 \times 10^{-8}$ s while the charging relaxation time of dust particle with the same radius is of order microseconds in glow discharge plasma sheath (Nitter 1996). It is thus clear that dust particles in fusion circumstances are charged in a much shorter time than in a glow discharge plasma sheath. Figure 5 also shows that the charging relaxation time of a dust particle becomes shorter as the κ value is increased. This is due to the fact that the increase of the κ value causes the decrease of the characteristic time of a dust particle, according to (3.8). Moreover, in the quasi-stationary state, the charge number of a dust particle increases significantly while the fluctuation of the dust particle charge changes a little. At the plasma-sheath edge, the RF oscillatory electric field caused by the applied current disturbance source becomes very small, and then the fluctuation of dust particle charge almost disappears. The charge number of the dust particle decreases as the κ value is decreased. This tendency is in agreement with the effect of the supra-thermal electrons on the charge number of the dust particle in a static sheath (Zhao *et al.* 2020).

To further discuss the effect of the supra-thermal electrons on the dust particle charge, we tabulate the quantities such as $\langle Z_d \rangle$, Z_d^{RMS}, Z_d^{RMSE} and $\Delta Z_d^{\mathrm{amp}}$ in table 1. For the variation of these quantities with the κ value, it is confirmed that the decrease in the supra-thermal electrons can cause a significant increase in the charge number of the dust particle, while causing a slight increase in the fluctuation of the dust particle charge for a dust particle with $r_d = 10\ \mu$m because $\omega_{\mathrm{ch}} = 1/\tau_{\mathrm{ch}} \propto r_d/\alpha$ increases within a narrow range, as indicated in figure 4.

As shown in figure 5, the opposite effect of the κ value on the dust particle charge near the sheath–wall interface and in the plasma-sheath edge can be found. To display the dependence of the dust particle charge modified by the κ value on the position in the sheath, we plot the profiles of the time-averaged dust particle charge in the quasi-stationary

	$\langle Z_d \rangle /10^4$	$Z_d^{\mathrm{RMS}}/10^4$	$Z_d^{\mathrm{RMSE}}/10^4$	$\Delta Z_d^{\mathrm{amp}}/10^4$
$\kappa = 3$	4.8626	4.8741	0.3352	0.4891
$\kappa = 5$	12.2842	12.2889	0.3407	0.5000
$\kappa = 10$	17.1445	17.1481	0.3530	0.5201

TABLE 1. Quasi-stationary state values in figure 5.
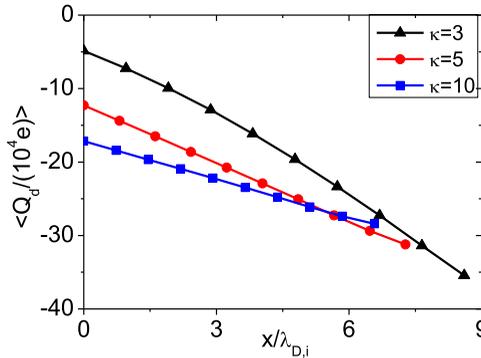
FIGURE 6. The profile of the time-averaged dust particle charge in the quasi-stationary state as a function of distance from the wall for the different κ values with $r_d = 10\,\mu$m. At the plasma-sheath edge positions $d_s/\lambda_{D,i}$: $8.6(\kappa = 3)$, $7.3(\kappa = 5)$, $6.6(\kappa = 10)$.

state as a function of distance from the sheath–wall interface for the different κ values in figure 6. It is found that the charge number of the dust particle increases from near the sheath–wall interface to the plasma-sheath edge. For the small κ value, the increase of the charge number is faster than for the large κ value. At the plasma-sheath edge, the charge number becomes larger than for the small κ value. This is the result of the effect of the supra-thermal electrons on the sheath structure. Near the sheath–wall interface, a strong RF field is formed due to the applied current disturbance source at the wall and the ion current at the wall is balanced mainly by the sum of the displacement and the disturbance current (Ou *et al.* 2019). The smaller κ value causes a larger sheath potential drop, as indicated in figures 2 and 3, and then electron density becomes smaller while the ion flux does not change so much. As a result, the dust particle potential drop decreases as the κ value is increased to keep the current from the plasma to the dust particle balance. At the plasma-sheath edge, the profiles of the plasma affected by the RF field is small, and the effect of the supra-thermal electrons on the dust particle charge is very similar to results obtained in a static sheath.

According to (3.8), the characteristic charging time, or the characteristic charging frequency, depends on the dust particle radius and supra-thermal electrons. To reveal the interplay of the supra-thermal electrons and dust particle radius on the dust particle charging process, figure 7 shows the variation of the mean charge of the dust particle and fluctuation of the dust particle charge in a quasi-stationary state with the κ value and r_d. It is demonstrated that the mean charge of the dust particle depends strongly on both κ and r_d, and a significant increase of $\langle Z_d \rangle$ can be found with the increase of both κ and r_d. The fluctuation of the dust particle charge increases with r_d, while it varies a little with the κ value. It must be mentioned that the dust particle charge depends obviously on r_d since the
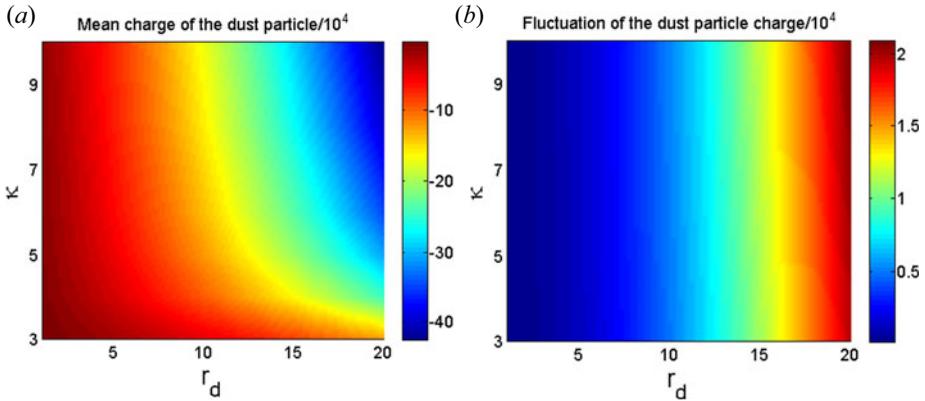
FIGURE 7. The mean charge of the dust particle $\langle Q_d \rangle$ (a), and fluctuation of the dust particle charge ΔZ_d^{amp} (b) near the sheath–wall interface in the quasi-stationary state as the functions of the κ value and r_d.

dust particle charge is nearly proportional to the dust particle radius, but the dependence of the dust potential drop on r_d may be very small in the quasi-stationary state according to (3.2)–(3.4). In figure 8, it is shown that the variations of the dust particle potential are almost the same for different radii of the dust particle, while the fluctuation of the dust particle potential increases with the dust particle radius under the same κ value conditions. For comparison, the values of $\langle \varphi_d \rangle$, φ_d^{RMS}, φ_d^{RMSE} and $\Delta \varphi_d^{amp}$ are tabulated in table 2 in the quasi-stationary state for the cases associated with figure 8. It is found that the dust particle potential drop is almost independent of the dust particle radius, but fluctuation of the dust particle potential increases with the dust particle radius. Moreover, φ_d^{RMSE} and $\Delta \varphi_d^{amp}$ are comparable for dust particles with small and large radii. Excepting $\Delta \varphi_d^{amp}$ for the large dust particle, our results are in good agreement with the results obtained in previous work (Shotorban 2012) within an order of magnitude. The main reason causing the difference of $\Delta \varphi_d^{amp}$ for the large dust particle may be the ratio of ω_{ch} and ω_{RF} (Melandsø *et al.* 1996). In our cases, because ω_{ch} is comparable to ω_{RF}, the dust particle charge only partially follows the RF field and has some time delay during an RF period, so $\Delta \varphi_d^{amp}$ increases but not much for the large dust particle. While for the case of $\omega_{ch} \gg \omega_{RF}$ presented by Shotorban (2012), the dust particle has enough time to change its charge during an RF period, and then $\Delta \varphi_d^{amp}$ increases an order of magnitude when the radius of the dust particle increases an order of magnitude. From the variation of φ_d^{RMSE} and $\Delta \varphi_d^{amp}$ with the κ value in table 2, it is also deduced that the fluctuation of the dust particle charge modified by the κ value depends on the dust particle radius and the effect of the κ value on the fluctuation of the dust particle charge becomes obvious for the large dust particle, since ω_{ch} or τ_{ch} for a change in Q_d is equal to the characteristic time for a change in φ_d (Melandsø *et al.* 1996).

In the investigation of the dust particle charging process in an RF sheath, the time-averaged instead of instantaneous plasma parameters are used to calculate the dust particle charge under some conditions, if the exact shape of the dust particle potential variation during the RF period it not taken into account (Nitter 1996; Hou *et al.* 2003; Bacharis *et al.* 2010; El Kaouini *et al.* 2014). To compare the difference of the dust particle charge obtained from the instantaneous plasma parameters and that obtained from the time-averaged plasma parameters in the non-Maxwellian electron sheath, we plot the evolution of the dust particle charge with time near the sheath–wall interface for instantaneous and time-averaged plasma parameters in figure 9. The dashed line denotes
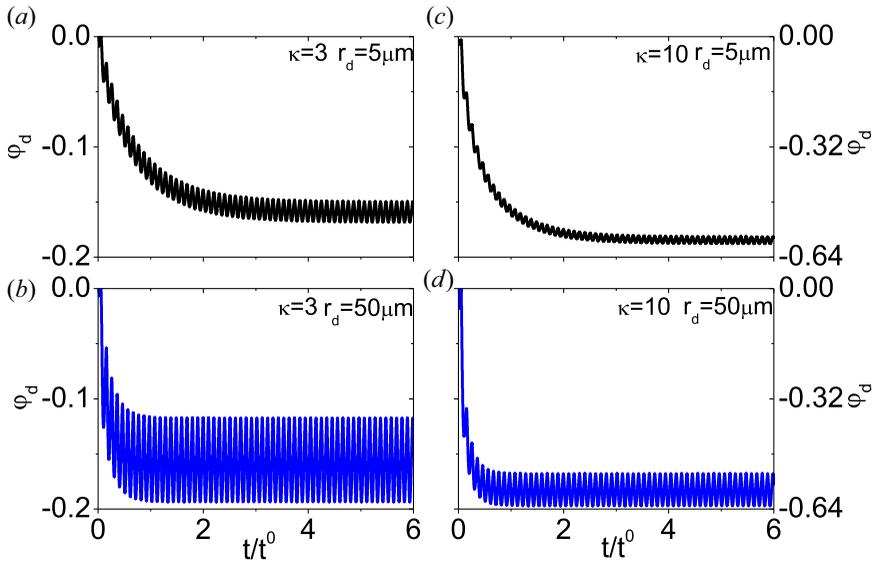
FIGURE 8. The evolution of the dust particle potential as a function of time for $\kappa = 3, \ r_d = 5 \ \mu m$ (a), $\kappa = 3, \ r_d = 50 \ \mu m$ (b), $\kappa = 10, \ r_d = 5 \ \mu m$ (c) and $\kappa = 10, \ r_d = 50 \ \mu m$.

	$|\varphi_d|$	φ_d^{RMS}	φ_d^{RMSE}	$\Delta\varphi_d^{\text{amp}}$
$\kappa = 3, \ r_d = 5 \ \mu m$	0.1598	0.1599	0.0064	0.0093
$\kappa = 3, \ r_d = 50 \ \mu m$	0.1587	0.1609	0.0261	0.0382
$\kappa = 10, \ r_d = 5 \ \mu m$	0.5916	0.5916	0.0069	0.0102
$\kappa = 10, \ r_d = 50 \ \mu m$	0.5880	0.5888	0.0317	0.0469

TABLE 2. Quasi-stationary state values in figure 8.

$\bar{Q}_d$ obtained from the time-averaged plasma parameters in the sheath. The dust particle charge obtained from the instantaneous plasma parameters is seen to oscillate with the RF frequency and is followed by the dashed line closely for the different κ values. However, the deviation degree of the dashed line in the quasi-stationary state increases with the decrease of the κ value. It is indicated that for the case of the time scale of the dust particle motion in the sheath being much longer than the RF period, it is good approximation to calculate the dust particle charge by using the time-averaged plasma parameters in the sheath of a Maxwellian plasma, and the difference of dust particle charge obtained from between instantaneous and the time-averaged plasma parameters increases as the supra-thermal electron population is increased. Based on figure 9, we tabulate the values of $\bar{Z}_d(\bar{Z}_d = |\bar{Q}_d/e|)$, $\langle Z_d \rangle$ and mean deviation $Z_d^{\text{MD}} = |(\langle Z_d \rangle - \bar{Z}_d)/\langle Z_d \rangle|$ in table 3 in the quasi-stationary state. We can see that the mean deviation of the charge number of a dust particle obtained from the time-averaged and instantaneous plasma parameters decreases as the κ value is increased, and the mean deviation always decreases for the larger dust particle under the same κ value conditions.
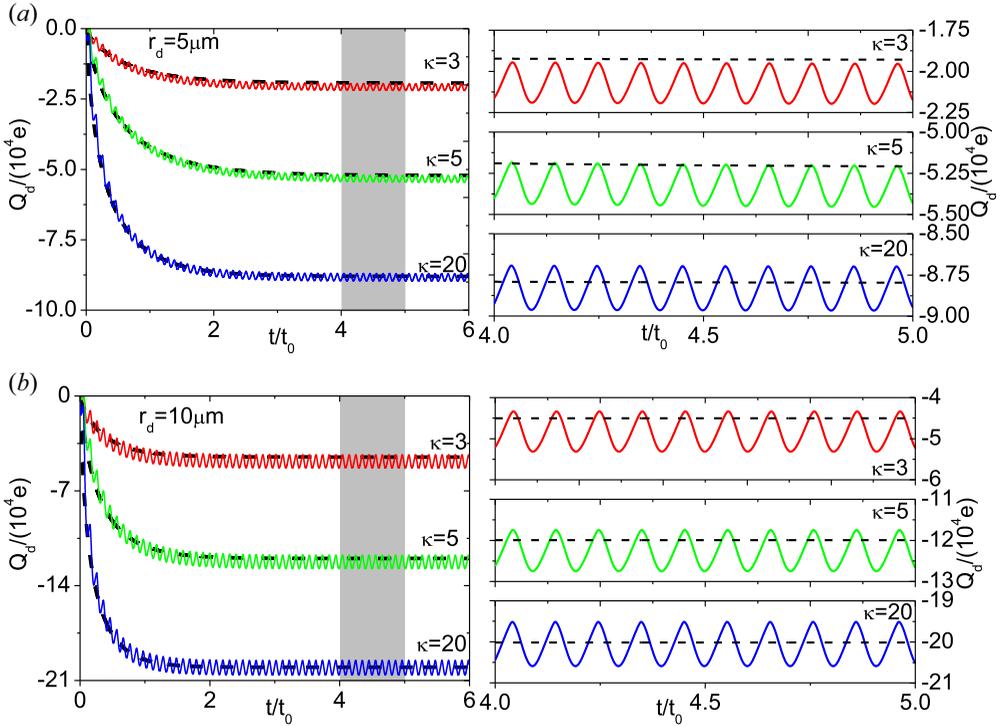
FIGURE 9. The evolution of the dust particle charge as a function of time for different κ values with $r_d = 5$ μm (a) and $r_d = 10$ μm (b). The dashed line denotes $\bar{Q}_d$ obtained from the time-averaged plasma parameters in the sheath.

	$\bar{Z}_d/10^4$	$\langle Z_d \rangle/10^4$	$Z_d^{MD}/10^4$
$\kappa = 3$, $r_d = 5$ μm	1.9316	2.0869	0.0744
$\kappa = 3$, $r_d = 10$ μm	4.5046	4.8626	0.0736
$\kappa = 5$, $r_d = 5$ μm	5.2170	5.3454	0.0240
$\kappa = 5$, $r_d = 10$ μm	11.9951	12.2842	0.0236
$\kappa = 20$, $r_d = 5$ μm	8.7989	8.8439	0.0051
$\kappa = 20$, $r_d = 10$ μm	20.0179	20.0963	0.0039

TABLE 3. Quasi-stationary state values in figure 9.

4. Conclusion

In the framework of a one-dimensional dynamical model of a non-Maxwellian plasma RF sheath, the effect of the supra-thermal electrons on the dust particle charging process is studied theoretically by taking into account the collection of electrons and ions from the plasma. In the sheath model, the non-Maxwellian electrons are assumed to obey the kappa distribution in which the parameter κ characterizes the deviation from a Maxwellian distribution, and the RF field is formed due to the applied current disturbance source at the wall in ICRF. By changing the κ value, we have obtained self-consistently the influence of the supra-thermal electrons on both the instantaneous and time-averaged

spatial distributions of some physical quantities in the sheath, such as the ion and electron densities and the ion velocity, which determine the dust particle charging process.

As the κ value is decreased, our results show that the charge number of a dust particle decreases near the sheath–wall interface while it increases near the plasma-sheath edge. Due to the strong RF field near the sheath–wall interface, significant oscillation of the dust particle charge with time can be found. The fluctuation of the dust particle charge increases with the κ value, and the increase caused by the κ value depends on the dust particle radius. For the small dust particle, the κ value impacts weakly on the dust particle charge, and its impact increases with the dust particle radius. From the comparison of the dust particle charge obtained from instantaneous and time-averaged plasma parameters, it is demonstrated that the relaxation process of the dust particle calculated from time-averaged plasma parameters follows the tendency obtained from the instantaneous plasma parameters, but the corresponding dust particle charge in the quasi-stationary state deviates from the result obtained from the instantaneous plasma parameters as the κ value is decreased. For the various κ values, the deviation always decreases when the dust particle radius becomes large.

Declaration of interests

The authors report no conflict of interest.

Funding

Data availability statement

The data that support the findings of this study are available from the corresponding author upon reasonable request.

REFERENCES

ABID, A.A., ALI, S. & MUHAMMAD, R. 2013 Dust grain surface potential in a non-Maxwellian dusty plasma with negative ions. *J. Plasma Phys*. **79**, 1117.

AUSSEMS, D.U.B., KHRAPAK, S.A., DOĞAN, İ, VAN DE SANDEN, M.C. & MORGAN, T.W. 2017 An analytical force balance model for dust particles with size up to several Debye lengths. *Phys. Plasmas* **22**, 062507.

BACHARIS, M., COPPINS, M. & ALLEN, J.E. 2010 Dust grain charging in RF discharges. *Plasma Source Sci. Technol*. **19**, 025002.

BEADLES, R., WANG, X. & HORANYI, M. 2017 Floating potential measurements in plasmas: from dust to spacecraft. *Phys. Plasmas* **24**, 023701.

EDELBERG, A. & AYDIL, E.S. 1999 Modeling of the sheath and the energy distribution of ions bombarding rf-biased substrates in high density plasma reactors and comparison to experimental measurements. *J. Appl. Phys*. **86**, 4799.

EL GHANI, O., DRIOUCH, I. & CHATEI, H. 2019 Effects of non-extensive electrons on the sheath of dusty plasmas with variable dust charge. *Contrib. Plasma Phys*. **59**, e201900030.

EL KAOUINI, M., CHATEI, H. & BOUGDIRA, J. 2014 Dynamics of dust particles in a collisional radio-frequency plasma sheath. *Phys. Scr*. **T161**, 014052.

FOROUTAN, G. & AKHOUNDI, A. 2012 Simulation study of the sheath region of a processing plasma with two-temperature electrons and charged nanoparticles. *Phys. Lett.* A **376**, 2244-2251.

HELLBERG, M.A., MACE, R.L., BALUKU, T.K., KOURAKIS, I. & SAINI, N.S. 2009 Comment on "Mathematical and physical aspects of Kappa velocity distribution" [Phys. Plasmas 14, 110702(2007)]. *Phys. Plasmas* **16**, 094701.

HOU, L., WANG, Y. & MISKOVIC, Z.L. 2003 Induced potential of a dust particle in a collisional radio-frequency sheath. *Phys. Rev.* E **68**, 016410.

KHALILPOUR, H. & FOROUTAN, G. 2020 The effects of electron energy distribution function on the plasma sheath structure in the presence of charged nanoparticles. *J. Plasma Phys*. **86**, 905860206.

KRASHENINNIKOV, S.I., SMIRNOV, R.D. & RUDAKOV, D.L. 2011 Dust in magnetic fusion devices. *Plasma Phys. Control. Fusion* **53**, 083001.

MELANDSØ, F., NITTER, T., ASLAKSEN, T. & HAVNES, O. 1996 The dust direct current self-bias potential in a time varying plasma sheath. *J. Vac. Sci. Technol.* A **14**, 619.

MISSAOUI, A., EL KAOUINI, M. & CHATEI, H. 2021 Effect of driving frequency on dust particle dynamics in radiofrequency capacitive argon discharge. *J. Plasma Phys*. **87**, 905870212.

NITTER, T. 1996 Levitation of dust in RF and DC glow discharges. *Plasma Source Sci. Technol*. **5**, 93.

OU, J., AN, X. & MEN, Z.Z. 2019 The effect of the energy electrons on the collisionless fusion plasma sheath in ion cyclotron range of frequencies heating. *Phys. Plasmas* **26**, 123514.

OU, J. & HUANG, Y. 2020 Ion energy distribution in a radio frequency sheath of plasma with Kappa electron velocity distribution. *Contrib. Plasma Phys*. **61**, e202000108.

OU, J., ZHAO, X.Y. & LIN, B.B. 2018 Dust charging and levitating in a sheath of plasma containing energetic particles. *Chin. Phys.* B **27**, 025204.

PUSTYLNIK, M.Y., PIKALEV, A.A., ZOBNIN, A.V., SEMENOV, I.L., THOMAS, H.M. & PETROV, O.F. 2021 Physical aspects of dust-plasma interactions. *Contrib. Plasma Phys*. **61**, e202100126.

QIN, C., ZHANG, X., ZHAO, Y., WAN, B., FRANZ, B., WANG, L., YANG, Q., YUAN, S., CHENG, Y. & ICRF TEAM ON EAST 2015 Electromagnetic analysis of the EAST 4-Strap ICRF antenna with HFSS code. *Plasma Sci. Technol*. **17**, 167.

SAMARIAN, A.A. & JAMES, B.W. 2001 Sheath measurement in rf-discharge plasma with dust grains. *Phys. Lett.* A **287**, 125.

SHOTORBAN, B. 2012 Stochastic fluctuations of dust particle charge in RF discharges. *Phys. Plasmas* **19**, 053702.

WHIPPLE, E.C. 1981 Potentials of surfaces in space. *Rep. Prog. Phys*. **44**, 1197.

ZHANG, K., DING, R., PENG, J., YAN, R., CHEN, J., ZHU, D., LI, C. & SI, X. 2021 Characterization of dust collected in EAST after 2019 campaign. *Plasma Sci. Technol*. **23**, 075104.

ZHAO, X., ZHANG, B. & WANG, C. 2020 Dust charging and levitating in a magnetized plasma sheath containing superextensive electrons. *Phys. Plasmas* **27**, 062507.